

The performance characteristics of a piezoelectric ultrasonic dental scaler

Pecheva, Emilia; Sammons, Rachel; Walmsley, Anthony

DOI:

[10.1016/j.medengphy.2015.10.008](https://doi.org/10.1016/j.medengphy.2015.10.008)

License:

Creative Commons: Attribution-NonCommercial-NoDerivs (CC BY-NC-ND)

Document Version

Peer reviewed version

Citation for published version (Harvard):

Pecheva, E, Sammons, R & Walmsley, A 2016, 'The performance characteristics of a piezoelectric ultrasonic dental scaler', *Medical Engineering & Physics*, vol. 38, no. 2, pp. 199–203.
<https://doi.org/10.1016/j.medengphy.2015.10.008>

[Link to publication on Research at Birmingham portal](#)

Publisher Rights Statement:

Eligibility for repository: Checked on 20/4/2016

General rights

Unless a licence is specified above, all rights (including copyright and moral rights) in this document are retained by the authors and/or the copyright holders. The express permission of the copyright holder must be obtained for any use of this material other than for purposes permitted by law.

- Users may freely distribute the URL that is used to identify this publication.
- Users may download and/or print one copy of the publication from the University of Birmingham research portal for the purpose of private study or non-commercial research.
- User may use extracts from the document in line with the concept of 'fair dealing' under the Copyright, Designs and Patents Act 1988 (?)
- Users may not further distribute the material nor use it for the purposes of commercial gain.

Where a licence is displayed above, please note the terms and conditions of the licence govern your use of this document.

When citing, please reference the published version.

Take down policy

While the University of Birmingham exercises care and attention in making items available there are rare occasions when an item has been uploaded in error or has been deemed to be commercially or otherwise sensitive.

If you believe that this is the case for this document, please contact UBIRA@lists.bham.ac.uk providing details and we will remove access to the work immediately and investigate.

The performance characteristics of a piezoelectric ultrasonic dental scaler

E. Pecheva^{1*}, R.L. Sammons, A.D. Walmsley

School of Dentistry, University of Birmingham, St Chad's Queensway,

Birmingham B4 6NN, United Kingdom

* tel. +44 121 4665545, fax +44 121 4665481, e.v.pecheva@bham.ac.uk (corresponding author)

¹ Permanent address: Laboratory of Biocompatible Materials, Institute of Solid State Physics, Bulgarian Academy of Sciences, 72 Tzarigradsko Chaussee blvd., 1784 Sofia, Bulgaria, emily@issp.bas.bg

Abstract

The objective of this work was to investigate the performance characteristics of a piezoelectric ultrasonic dental scaler using scanning laser vibrometry. The vibration characteristics of three standard piezoelectric tips were assessed with scanning laser vibrometry under various conditions: unconstrained, under a stream of flowing water, in a water tank, as well as subjected to loads to simulate clinical conditions. Subsequently, the tips were used to disrupt an in-vitro biofilm model of dental plaque, developed using a non-pathogenic Gram-negative species of *Serratia* (NCIMB40259).

The laser vibrometry data showed that the oscillation pattern of the ultrasonic tip depends primarily on its shape and design, as well as on the generator power. Thin tips and high power settings induce the highest vibrations. Water irrigation of the tip and loads influence the tip performance by diminishing its vibration, while water volume increases it.

Serratia biofilm was disrupted by the cavitation bubbles occurring around the scaler tip. The most effective biofilm removal occurred with the thinner tip.

Understanding how the ultrasonic tip oscillates when in use and how it removes dental plaque is essential for gaining more knowledge regarding the cleaning mechanisms of the ultrasonic system. Cavitation may be used to remove plaque and calculus without a mechanical contact between the dental tip and the teeth. Better knowledge would enable dental specialists to understand and improve their techniques during routine cleaning of teeth. It will also lead to improving tip design and to the production of more effective instruments for clinical use.

Key words: scanning laser vibrometry, ultrasonic scaler, vibration performance, displacement, cavitation, biofilm disruption

1. Introduction

When using ultrasonic scalers, the debridement of plaque and calculus is primarily achieved by the mechanical chipping action of the scaler tip [1-3]. A stream of water flows over the tip to prevent frictional heating and to wash debris from the treatment site. It was found that cavitation bubbles are generated in the water around the oscillating ultrasonic scaler tip [4,5]. One effect that cavitation causes is the breakdown of water molecules and hence the production of reactive species inside the cavitation bubbles [6,7]. In addition, microstreaming occurs and it impacts on a surface thus aiding the surface cleaning [8,9]. Recently it has been proposed that ultrasonic scaler debridement involves the use of the cavitation bubbles as another mechanism to remove plaque and calculus from teeth surface, periodontal pockets and dental implants and may lead to advances in enhancing the cleaning process [9-11].

An appreciation of the movement of ultrasonic scalers would enable dental specialists to understand and improve their techniques during routine teeth cleaning. The oscillations of ultrasonic tips have been successfully assessed using a novel technique, namely scanning laser vibrometry (SLV), providing a more detailed understanding of the way in which factors such as constraint, load and wear affect scaler vibrations and hence its performance [12,13]. These papers proved a useful insight into the oscillation of the tips, however newer piezoelectric generators have entered the market which have different shapes to those previously evaluated.

This paper aims to assess the vibration motion of a piezoelectric ultrasonic scaler with different shaped tips ranging from broad based shape to those which resembled a thin probe shape for better accessing periodontal pockets. These were assessed under simulated clinical conditions to determine which factors lead to the greatest influence on the

movement. In addition, the disruption of a bacterial biofilm representing the dental plaque was studied to explore the action of assumed cavitation bubbles around the ultrasonic tip.

2. Materials and Methods

2.1. Tip design and measurement settings

A piezoelectric dental scaler (Satelec P5XS Newtron, Acteon, France, 30 kHz) was selected for this study with three tips of different designs (Fig. 1a) used by dental specialists to access subgingival pockets [10]. Tips 1 and 2 had rectangular cross-section and tip 2 was broader than tip 1. Tip 10P had circular cross-section and it was the thinnest, and the longest tip. Tips were handmade of stainless steel and before the analysis and experiments they were cleaned with ethanol. The analysis of tip vibrations was performed under unconstrained and unloaded conditions in air (Fig. 1b). Subsequently, the oscillating tips were put under constrained conditions by adding water either as a flow from a small outlet on the back of the tip, running over its body at a constant rate of 30 ml/min (Fig. 1c), or in a water tank containing 50 ml of distilled water (Fig. 1d). Finally, tips were tested against a plastic tooth attached to a digital balance (Timetop, capacity 1000 g, precision 0.1 g) and loads from 10 g to 150 g were applied towards the front side of the tip during its vibration (Fig. 1e); the contact was made at the free end of the oscillating tip (final 1 mm).

2.2. Scanning laser vibrometry analyses

The vibration analyses of the scaler tips were performed using a SLV high frequency scanning vibrometer system (PSV 300-F/S, Polytech GmbH, Waldbronn, Germany), which works with an eye-safe He-Ne laser ($\lambda=632.8$ nm, class 2). The principle of SLV measurement has been discussed previously [14,15]. A frequency measurement range of 0-

100 kHz was selected to allow detection of the fundamental frequency of the scaler, as well as higher order harmonics. The SLV was set to perform fast Fourier transformation using 800 data points, giving a frequency resolution of 125 Hz thus enabling both the longitudinal and lateral oscillation pattern of the tip to be accurately determined. The laser beam was focused at the tip free end as shown in Fig. 1b and a number of equally-spaced scan points were chosen along the tip length, from the free end to as close to the handpiece as could be measured. The handpiece was clamped so that the tip was vertical and clearly visible to the SLV camera. Full characterisation of the unconstrained tip vibrations was performed with the laser beam focused on the front, back and side of the tip. The maximum tip displacement at each scan point was measured and an average of 5 measurements was recorded for each tip, at each power setting (1-lowest to 20-highest). Each scan lasted approximately 10 s with an interval of 20 s between scans.

2.3. Bacterial biofilm formation and its disruption

An in-vitro biofilm model system using a non-pathogenic Gram-negative species of *Serratia* (NCIMB40259) has been developed in a bioreactor [16]. *Serratia* is capable of forming biofilm on various surfaces and also mineralising it to calcium deficient hydroxyapatite that chemically resembles calculus and has a similar tenacity on surfaces [16]. The bacterial biofilm with thickness of about 2 μm was grown on microscope glass slides (20x10x1 mm) and titanium disks (Ti; diameter 15 mm). The irrigated dental tip was placed parallel to the biofilm-coated materials with their front side and tip end facing down. Then the ultrasonic scaler has been operated for 30 sec at a fixed power setting, giving a tip displacement of 15 μm . Direct mechanical contact of the tip with the materials was avoided by placing them at a distance of 40 μm . To extract the effect of water

impingement on the biofilm disruption, a stream of water from a 50 ml syringe placed at 1 or 5 mm distance to the Ti and glass surfaces was directed to the biofilm.

2.4. Statistical analysis

SLV data from the scan point located at the unconstrained end of the tips were analysed using IBM SPSS v.21 for Windows (SPSS Inc., Chicago, IL, USA). The significance of variation in the maximum tip displacement amplitude at different generator power settings, as well as under various constraints and load conditions was tested using univariate analysis of variance (ANOVA, general linear model) and multiple post hoc comparisons (Tukey test). For similar studies the significance level is set as $p < 0.05$ with the dependent variable being the displacement amplitude.

3. Results

The SLV data is presented as the maximum displacement amplitudes along the length of the unconstrained tip and the scans revealed one node at about 3.5 mm (tips 1 and 2) or 4.5 mm (tip 10P) measured from the tip free end (Fig. 2a). Two antinodes could be identified: at the very end of the tips (first scan point; position A in Fig. 1a) and at about 6.5 mm, 5.0 mm or 8.5 mm for tips 1, 2 and 10P, respectively (position B in Fig. 1a). Displacement clearly increased with increasing power from the lowest (1) to the maximum generator power (20). There was an over-range signal when recording the tip end at the highest power settings. Tip 2 exhibited the lowest displacements whilst tip 1 gave higher amplitudes of oscillation. Tip 10P had the highest vibrations at all power settings. Side vibrations were also assessed (Fig. 2b) and they consisted of displacements of about 10% of the values measured for the front of tips 1 and 10P and 5% for tip 2 at high power

settings (15 and 20).

Tip oscillations under water flow were compared to those in air (Fig. 3) and it was found that the displacement amplitude decreased for both the tip front and back when water flow was present. At average power setting (10) the water flow decreased the tip 10P vibrations. Contrary to the effect of the irrigation, when water was used as a volume constraint, the vibrations of the three tips were unambiguously higher at settings 1 to 10 than in air for both measurements of the tips front and back, with tip 2 showing the most stable behaviour for all power settings.

The maximum displacement amplitude at the tip free end under various loads was plotted as a function of the generator power settings (Fig. 4). The amplitude steadily decreased for all three tips with increasing load from 10 g to 150 g. Tip 2 had the most stable behaviour upon loading and yielded the lowest displacement values. Difficulties in measuring the displacement at the highest power were experienced for tip 1 at 100 g and 150 g, and especially for the thinnest tip 10P at all loads. The increase of the generator power yielded a linear increase in the displacement amplitude with the maximum value measured for setting 15.

Analysis of vibration data from the unconstrained end of all tips showed that power settings, environmental conditions and position of measurement were statistically significant variables ($p=0.000$). Low (1, 5) and average (10) power settings were different from high (15, 20) power settings ($p=0.001$) while settings 15 and 20 were not different ($p=1.000$). Displacements of tips 1 and 2 in air and water flow were different from those in the water tank ($p=0.0001$) and vibrations measured from the front and back of tips 1 and 2 were different from those from the side ($p=0.000$). Post hoc comparison for tip 10P revealed differences for power settings 1 and 5 ($p=0.0001$), while no differences were found for power setting 10 to 15 ($p=0.997$), 10 to 20 ($p=0.717$) and 15 to 20 ($p=0.886$).

Vibration data in air for tip 10P were significant from those under water flow ($p=0.006$) and in the water tank ($p=0.0001$), as well as the displacements measured from the front, back and side of this tip ($p=0.0001$).

When load was applied to the tip, significant difference was found for the loaded 1, 2 and 10P tips in comparison to unloaded conditions ($p=0.0001$). Tip vibrations due to loads > 70 g were also found different. A Tukey test for the three tips showed that tip and power settings were significant variables ($p=0.000$).

With the knowledge gained about the vibration movement of the three tips, we further used them to disrupt the *Serratia* biofilm grown on Ti and glass. Representative images of the biofilm after disruption showed that the most effective removal on both materials occurred with the thinner tips 1 and 10P, and the least effective with the broadest tip 2 (Fig. 5). When the tip was oriented side on, only their “contact footprint” was visible. There was no disruption with the tip placed perpendicularly and only the end in contact with the biofilm (not shown). The water impingement from a syringe also did not yield the formation of biofilm lesions on the Ti and glass surfaces. Since the vibrating scaler tip was placed at a distance of $40\text{ }\mu\text{m}$ to the biofilm and thus the mechanical chipping action was avoided, it was assumed that the cavitation bubbles cloud observed around the tip played a role in the *Serratia* biofilm disruption.

4. Discussion

When used for dental scaling, the ultrasonic scaler is set at an arbitrary value often being “tuned” by the operator to obtain the best sound before using the instrument on the patient. Previous work [10] has shown that there is variation with ultrasonic scalers and this may produce different clinical outcomes. The majority of studies do not perform a

basic test of the operating scaler. The tip may undergo a range of oscillatory movements depending on the tip being in air or water. The latter also leads to differences depending if immersed in water or if it is passed over it.

Using laser vibrometry it was possible to carry out detailed analyses of the oscillations of piezoelectric dental tips under different conditions (unconstraint, constraint by water flow or water volume and loaded). We could also observe the tip response to varying generator power, as well as to determine the locations of nodes and antinodes along the length of the scaler tip which is associated with the occurrence of cavitation [9] and thus can be related to the disruptive effect of the tip when approaching biofilms.

Performing unconstrained vibration measurements of ultrasonic tip (i.e. in air) gives a guide to the performance of the power generator driving the tip and also to the way in which the tip responds to changes in power. Previously the increase of power settings has led to the increase of the tip displacement values [14] and it was also confirmed in this study. Also, the vibrational antinode with the greatest displacement amplitude was found to always occur at the free end of the tip (position A in Fig. 1a).

Tip design is influential in determining the tip vibrations [9,12]. Tips 1 and 2 had a flat cross-section and tip 2 was broader than tip 1. Tip 10P had a circular cross-section, it was thinner and longer than the other two tips (Fig 1a). The broadest tip 2 had the lowest displacement values and the most stable vibration motion while tips 1 and 10P are thinner and had higher amplitudes of oscillation (Figs. 2-4) especially the longest, 10P. Even though thinner tips are preferred in clinics because they enable easier access to tooth roots, the cavitation occurrence around thin tips may be reduced when used in areas with difficult access [9,15].

This study resembled the clinical situation where irrigation liquid or disinfectant water is flowing over the tip [9]. When the tip was vibrating under a water flow (Fig. 3),

the oscillations were suppressed in comparison to these in air.

The movement characteristics of the tip in a large water volume have not been reported previously. However, liquid volumes are also often used when imaging dental tip vibrations and resulting cavitation bubbles with high-speed cameras [6,9]. Contrary to the measurements with the water flow, tip vibrations in the water tank increased and the displacement values measured for the tip front and back were generally higher than these in water flow or in air (Fig. 3). We consider that this boosting effect was due to the presence of a water volume around the tip, larger than the tip volume, which acted as an amplifier. The effect was clearly pronounced for tip 2 at all power settings, for tip 1 up to setting 15 and for the back of tip 10P at all power settings. Clinically there will be much variation as the tip is rarely immersed fully in liquid unless working in the posterior part of the mouth. In the anterior region, the water flow is likely to move off the tip during usage.

The application of in-vitro load was also found to influence the vibration patterns [12]. All tip displacements at settings from 1 to 20 decreased steadily with the application of the lower loads (< 70 g), as well as when it was increased to clinical loads, i.e. > 100 g (approximately 1 N) (Fig. 4).

The degree of variability observed in the unconstrained and constrained vibrations of tips 1 and 10P might be due to several factors. One reason is when the energy of the working frequency is transferred to a harmonic frequency, which results in a decrease in the displacement amplitude measured for the fundamental frequency. Analysis of the frequency spectra obtained with the SLV software up to the second harmonic frequency revealed that this was probably not the case in this study. Other reasons could be variability in the behaviour of the piezoelectric handpiece driving the tip, which may arise because of differences in tightness of fit when they were screwed into position in the handpiece, even though care was taken to screw the tip correctly. Wearing out of the tip could also have been

a significant factor affecting the decrease of the oscillation amplitude. The SLV data obtained in this work gives us the opportunity to obtain better knowledge on tip motion in constrained and loaded environments. They will also allow dental specialists to understand better the cleaning mechanisms of the ultrasonic scalers and thus to improve their techniques during routine cleaning of teeth. It may also lead to improvements in tip design and to the production of more effective dental instruments for clinical use.

The second stage in our work was to assess the effect of the cavitation occurring around the vibrating ultrasonic tip on the disruption of *Serratia* biofilm used to model the dental plaque. A biofilm is any group of microorganisms sticking to each other and adhering on a surface and they are embedded within a self-produced matrix of extracellular polymeric substances [17,18]. Biofilms are involved in a wide variety of microbial infections in the body and dental diseases such as dental plaque and gingivitis are one of the infectious processes in which biofilms have been implicated in the oral cavity [19].

Cavitation bubbles around a scaler tip have been expected to remove plaque and calculus from teeth surfaces due to the shock waves produced upon their collapse [6,7,11]. *Serratia* biofilm provided a useful model for investigation of the efficacy of the ultrasonic dental scaler for plaque removal (Fig. 5). The three tips removed the biofilm on glass and Ti only when their front side was used and the tip sides or tip end did not yield a disruption area under the conditions used here. Tip width, position and angle all influenced the biofilm disruption. Simple experiment with water ejected from a syringe showed no biofilm lesions and thus excluded the possibility that the water flowing over the tip itself disrupted the biofilm. This means that the disruptive effect was due to the cavitation.

5. Conclusion

The oscillation pattern of each piezoelectric tip depends on the tip shape and design, as well as on the generator power. Additionally, irrigation water flowing over the tip and loads suppresses the tip vibration amplitudes while a large volume of water around the tip increases them. Clinical loads ($> 1\text{N}$) together with high power settings make the tip behave unpredictably. Non-contact biofilm disruption with the ultrasonic scaler involves the use of cavitation bubbles, which enhance the cleaning of plaque from the glass and titanium surfaces.

Acknowledgement

This work is funded by the Engineering and Physical Sciences Research Council of the United Kingdom (grant № EP/J014060/2013).

Competing interests: None declared

Ethical approval: Not required

References

- [1] Badersten A, Nilveus R, Egelberg J. Effect of non-surgical periodontal therapy. 1. Moderately advanced periodontitis. *J Clin Periodont* 1981;8:57–72.
- [2] Breininger DR, O’Leary TJ, Blumenshine RVH. Comparative effectiveness of ultrasonic and hand scaling for the removal of subgingival plaque and calculus. *J Periodont* 1987;58:9–18.
- [3] Loos B, Kiger R, Egelberg J. An evaluation of basic periodontal therapy using sonic and ultrasonic scalers. *J Clin Periodont* 1987;14:29–3.
- [4] Prosperetti A. Bubbles. *Physics of Fluids* 2004;16:1852–65.
- [5] Brennen CE. Cavitation and bubble dynamics. Oxford: Oxford University Press; 1995.
- [6] Verhaagen B. Root canal cleaning through cavitation and microstreaming (thesis). University of Twente, 2012.
- [7] Leighton TG. The acoustic bubble. London: Academic; 1994.
- [8] Henglein A. Chemical effects of continuous and pulsed ultrasound in aqueous solutions. *Ultrason Sonochem* 1995;2:S115–21.
- [9] Walmsley AD, Lea SC, Felver B, King DC, Price GJ. Mapping cavitation activity around dental ultrasonic tips. *Clin Oral Investig* 2013;17:1227–4.
- [10] Walmsley AD, Lea SC, Landini G, Moses AJ. Advances in power driven pocket/root instrumentation. *J Clin Periodont* 2008;35:22–8.
- [11] Rivas DF, Verhaagen B, Seddon J, Zijlstra A, Jiang LM, van der Sluis L, et al. Localized removal of layers of metal, polymer, or biomaterial by using ultrasound cavitation bubbles. *Biomicrofluidics* 2012;6:034114-20.
- [12] Lea SC, Felver B, Landini G, Walmsley AD. Three-dimensional analyses of ultrasonic scaler oscillations. *J Clin Periodont* 2009;36:44–0.

- [13] Lea SC, Felver B, Landini G, Walmsley AD. Ultrasonic scaler probe oscillations and tooth surface defects. *J Dent Res* 2009;88:229–4.
- [14] Lea SC, Landini G, Walmsley AD. Vibration characteristics of ultrasonic scalers assessed with scanning laser vibrometry. *J Dent* 2002;30:147–1.
- [15] Lea SC, Walmsley AD. Mechano-physical and biophysical properties of power-driven scalers: driving the future of powered instrument design and evaluation. *Periodont 2000* 2009;51:63-78.
- [16] Medina Ledo H, Thackray A, Jones I, Marquis P, Macaskie L, Sammons R, Microstructure and composition of biosynthetically synthesised hydroxyapatite. *J Mater Sci Mater Med* 2008;9:3419-27
- [17] Terminology for biorelated polymers and applications (IUPAC Recommendations). *Pure Appl Chem* 2012;84: 377–410
- [18] Hall-Stoodley L, Costerton JW, Stoodley P. Bacterial biofilms: from the natural environment to infectious diseases. *Nature Rev Microbiol* 2004;2:95–108
- [19] Rogers AH. *Molecular Oral Microbiology*. Caister Academic Press; 2008, p. 65–108.

Figure and Table captions

Figure 1 (a) Design of Satelec tips 1, 2 and 10P; the free end of the tip (position A) is placed side-on to the tooth during treatment. Tip vibrations are measured in air (b), under water flow (c), in water tank (d) and loaded (e).

Figure 2 (a) Maximum displacement amplitude (\pm SD, μm) along the length of the tip vibrating in air, plotted as a function of the distance from the tip unconstrained end.

(b) Comparison of the displacement amplitude (\pm SD, μm) measured for the front, back and side of the tip free end vibrating in air, plotted as a function of power settings.

Figure 3. Comparison of the effect of water constraint on the displacement amplitude (\pm SD, μm) of the tip free end (front side).

Figure 4. Comparison of the effect of loads on the displacement amplitude (\pm SD, μm) of the tip free end (front side).

Figure 5. Representative digital camera images of the *Serratia* biofilm disrupted with the tip front side: (a) Ti disk contacted with tip 2; (b) glass slide contacted with tip 1; (c) optical microscopy image of (b).

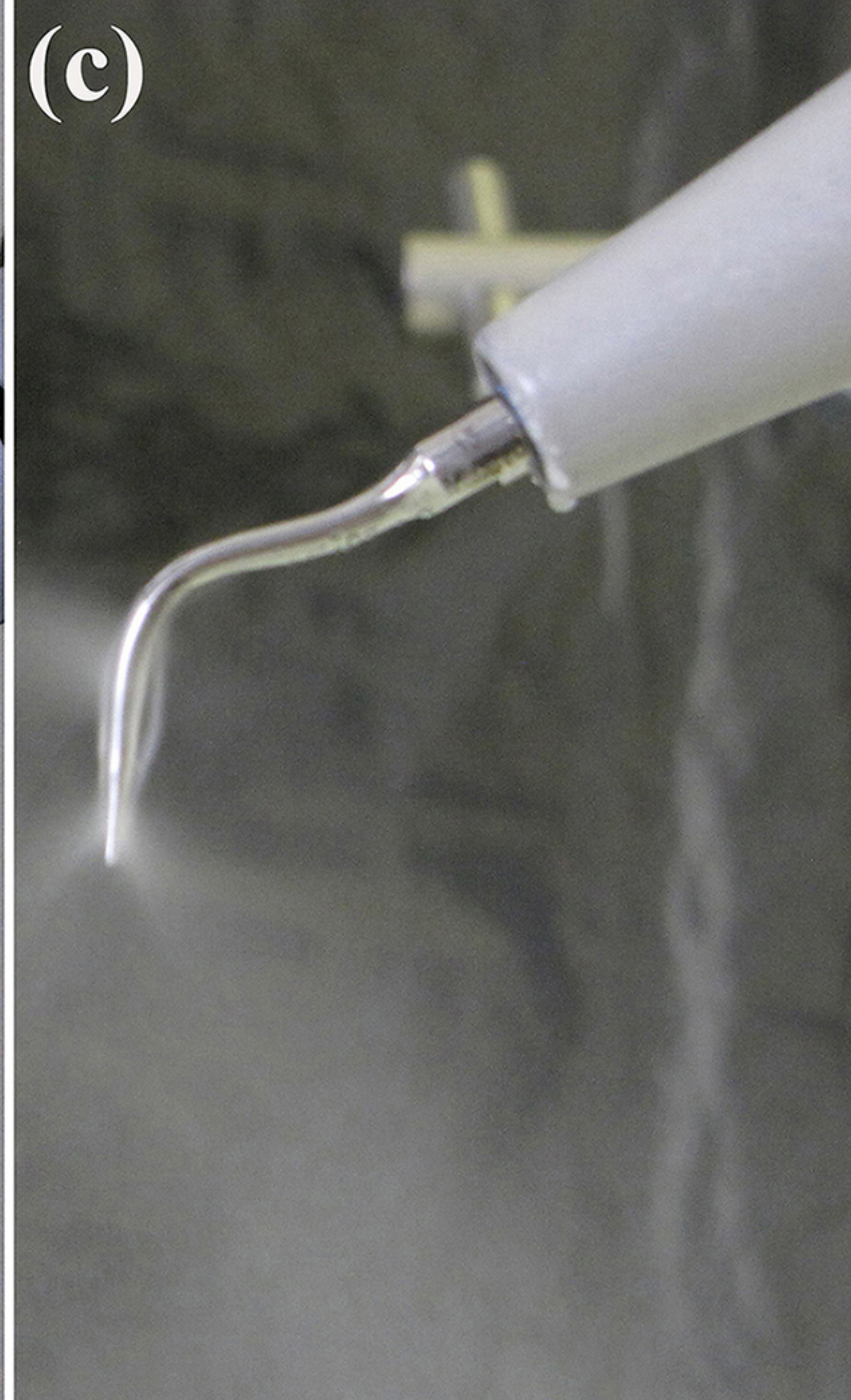
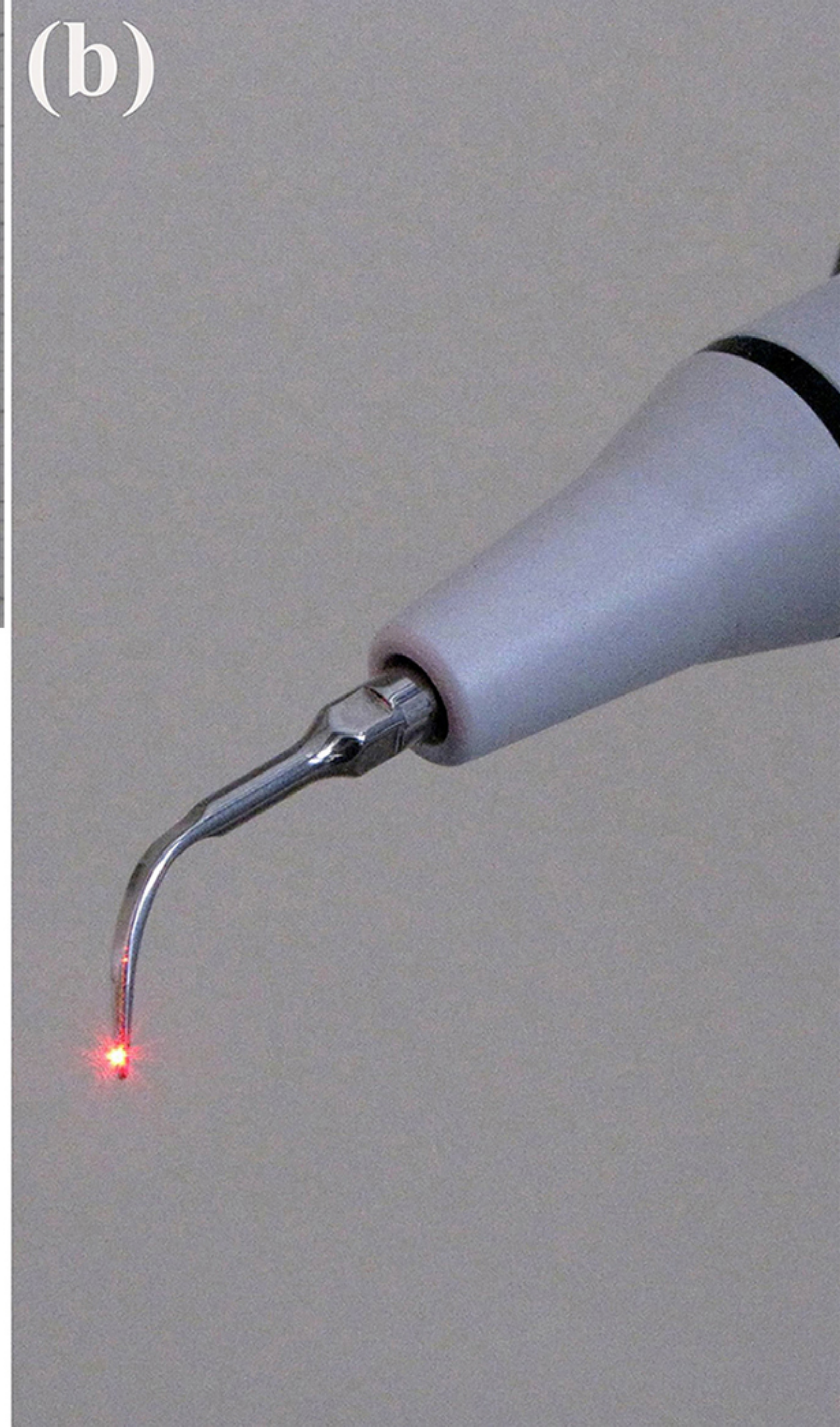
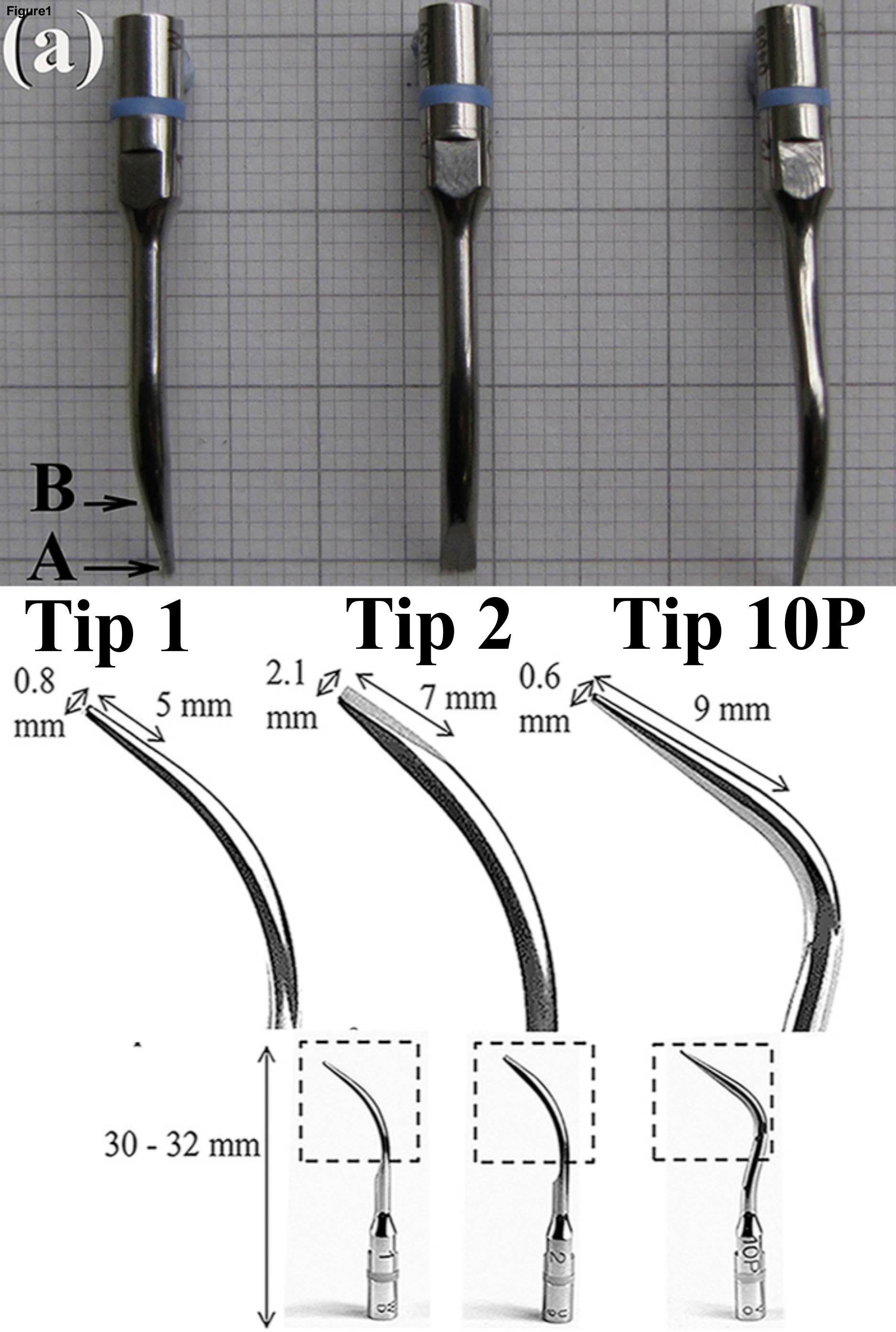


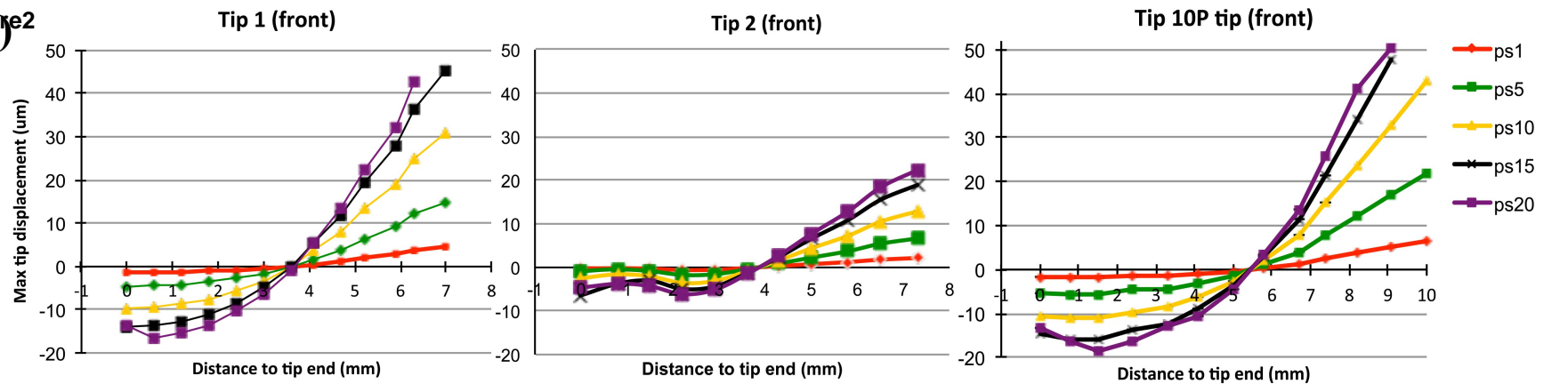
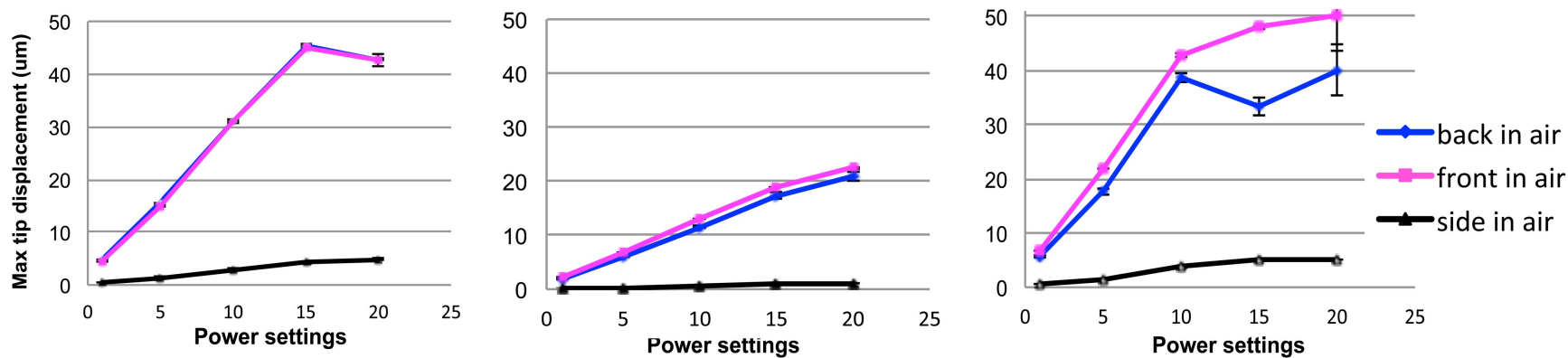
Figure 2
(a)**(b)**

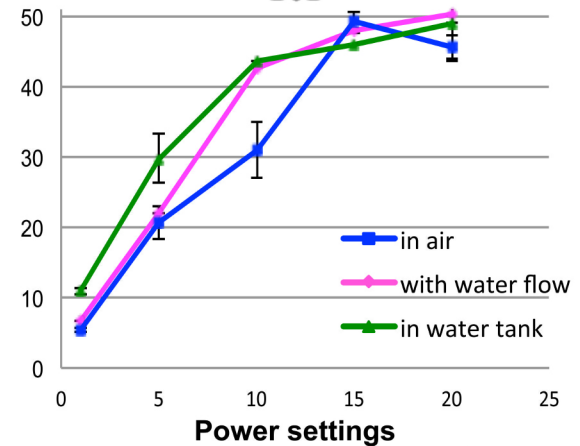
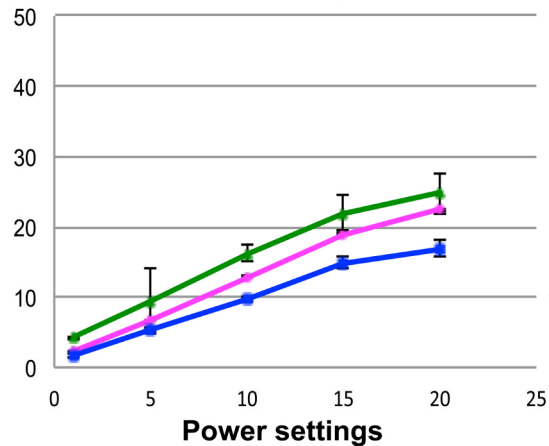
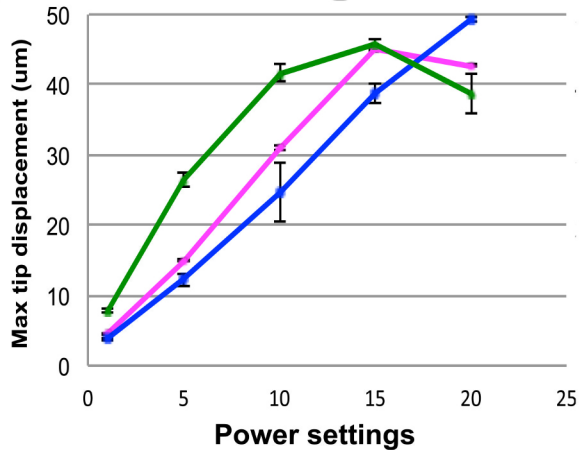
Figure3

Figure4

